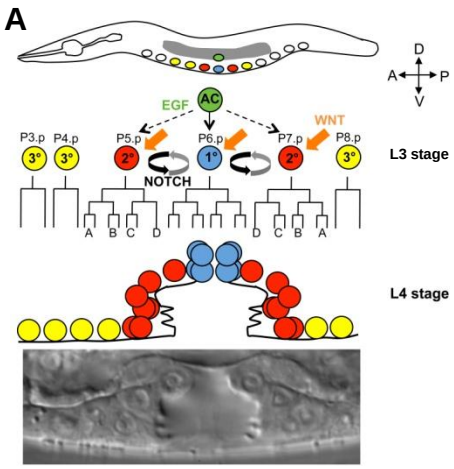

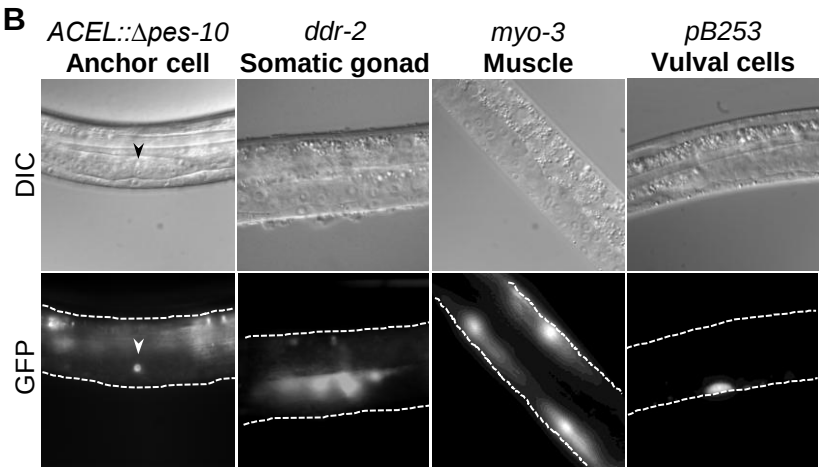

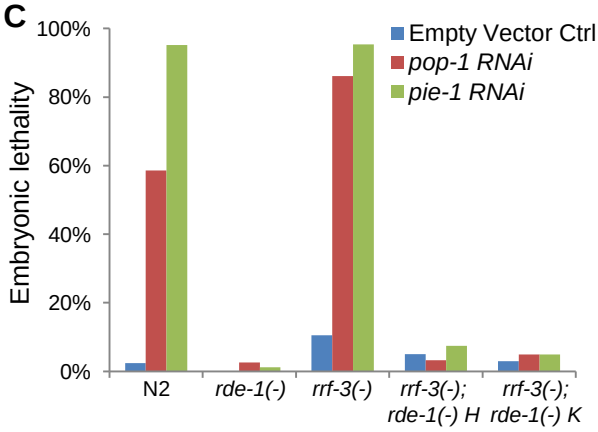

D

RNAi	rde-1(+)	rde-1(-)	Mesoderm-rde
lin-3	13/17 Vul 4/17 Partial Induction	20/20 Normal	10/28 Vul
lin-39	1/56 Normal 13/56 Partial induction 42/56 Vul	58/58 Normal	51/62 Normal 10/62 Partial induction 1/62 Vul

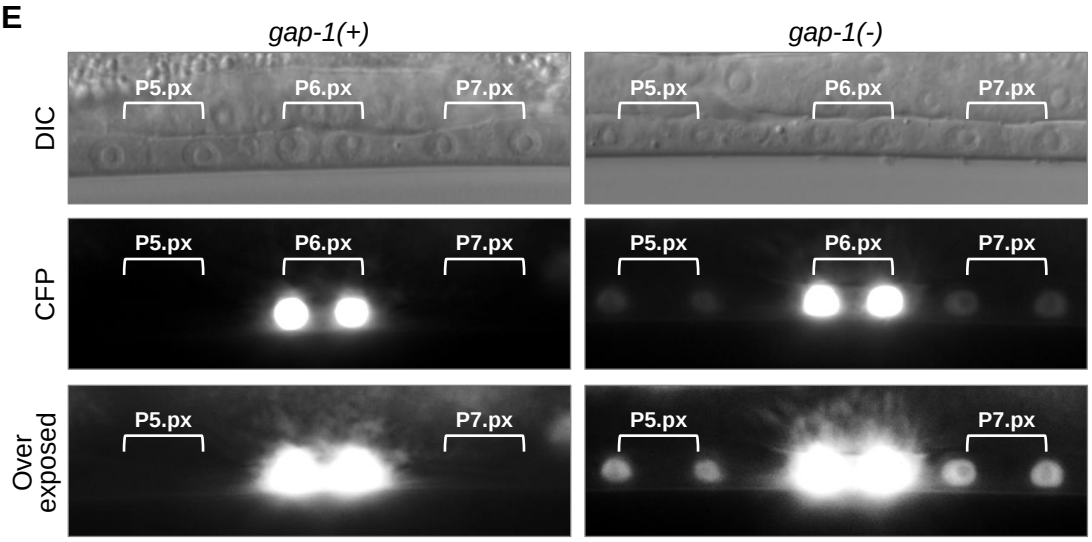

F

WormMart	# Genes	% Conserved	*p*-value
Total genes in RNAi library	16,256		
Conserved genes in RNAi library	7,670	47.2	
Identified mesodermal genes	39		
Conserved mesodermal genes	31	79.5	0.00007

Figure S1 related to Figure 1 and Figure 3. Mesodermal RNAi in *C. elegans* identifies conserved factors. **(A)** Schematic of vulva development**.** Top: circles depict VPCs and anchor cell (AC). Gonad is in gray. Middle: during larval L3 stage, signaling pathways frequently mutated in human cancer induce VPCs to divide to form the 22 cells of the mature vulva, a DIC image of which is shown at the mid-larval L4 stage (bottom). A, anterior; P, posterior; V, ventral; D, dorsal. Reproduced / adapted with permission from Green et al., *Development*, 2007. **(B)** DIC (top) and fluorescence (bottom) images of larval L3 transgenic worms expressing GFP driven by tissue-specific promoters active in the anchor cell (arrowhead), somatic gonad, muscle, and vulval cells. Dashed lines indicate worm body boundaries. **(C)** RNAi sensitivity was enhanced by introducing the *rrf-3* mutation (*rrf-3(-)*). Introduction of the *rrf-3(-)* allele did not inadvertently alter RNAi resistance of *rde-1(-)* strains because *rrf-3(-); rde-1(-)* double mutants were viable upon RNAi-mediated depletion of two essential genes, *pop-1* (TCF/LEF transcription factor) and *pie-1* (CCCH zinc finger protein). Embryonic lethality was evaluated in two independent *rrf-3(-); rde-1(-)* double mutant isolates, *H* and *K*. N2, wild-type. **(D)** Summary of Vulvaless phenotypes (Vul) after RNAi-mediated depletion of *lin-3* and *lin-39* in wild-type *rde-1* worms (*rde-1(+)*), *rde*-1 mutants (*rde-1(-)*) and *rde-1(-)* mutants with mesoderm-specific RNAi (*mesoderm-rde*). **(E)** DIC and fluorescence images of wild-type *gap-1* (*gap-1(+)*) and *gap-1*-mutant (*gap-1(-)*) worms expressing a LET-60/RAS-dependent transcriptional reporter. Cell lineages are designated as P6.px (presumptive 1° cell fate) and P5.px and P7.px (presumptive 2° cell fate). Bottom panels are overexposed to better visualize CFP expression in P5.px and P7.px cells. **(F)** Percentage of genes with mammalian orthologs for all *C. elegans* genes included in the RNAi library or the 39 mesodermal genes identified by the RNAi screen. P=0.00007, Fisher's exact test.

A

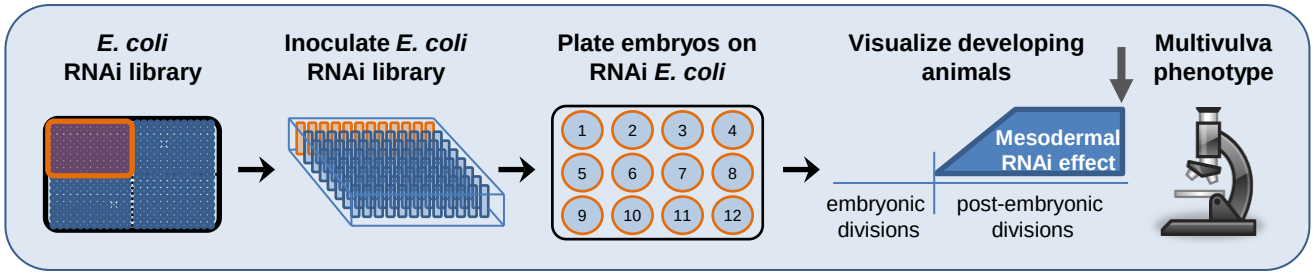

B

Chr. #	RNAi Library ID	*C. elegans* Gene	Human Ortholog	Gene Description
Chromatin Remodeling				
I	K07A1.11	*rba-1*	*RBBP4*	retinoblastoma binding protein 4
II	ZK131.9	*his-15*	*HIST2H2BF*	histone cluster 2, H2bf
III	Y49E10.6	*his-72*	*H3F3A/H3F3B*	histone H3.3
III	C07A9.3	*tlk-1*	*TLK1/TLK2*	tousled-like kinase 1/2
IV	F55G1.10	*his-61*	*HIST2H2AB*	histone cluster 2, H2ab
IV	T22D1.10	*ruvb-2*	*RUVBL2*	RuvB-like AAA ATPase 2
V	F45F2.3	*his-5*	*HIST1H4H*	histone cluster 1, H4h
V	C55A6.9	*C55A6.9*	*PAF1*	RNA polymerase II associated factor
Cytoplasmic Polyadenylation				
I	B0414.5	*cpb-3*	*CPEB1*	cytop. polyadenylation element binding protein 1
V	F25G6.2	*symk-1*	*SYMPK*	symplekin
Translational Regulation				
I	F26A3.2	*ncbp-2*	*NCBP2*	nuclear cap binding protein subunit 2, 20kDa
II	Y57A10A.30	*ife-5*	*EIF4E*	eukaryotic translation initiation factor 4E
IV	F55F10.1	*F55F10.1*	*MDN1*	MDN1, midasin homolog (yeast)
IV	Y51H4A.15	*Y51H4A.15*	*TSR2*	20S rRNA accumulation, homolog (*S. cerevisiae*)
V	D1054.15	*plrg-1*	*PLRG1*	pleiotropic regulator 1 (PRL1 homolog, *Arabidopsis*)
Other Functions				
I	W02D9.1	*pri-2*	*PRIM2*	primase, DNA, polypeptide 2 (58kDa)
II	K10G6.1	*lin-31*	*FOXB1*	Forkhead Box B1
II	R53.3	*egl-43*	*PRDM16*	PR domain containing 16
II	ZK430.1	*toe-1*	*HEATR1*	HEAT repeat containing 1
II	C56E6.1	*abcx-1*	*ABCG5*	ATP-binding cass., sub-family G (WHITE), mem. 5
III	F58A4.4	*pri-1*	*PRIM1*	primase, DNA, polypeptide 1 (49kDa)
III	T26G10.1	*T26G10.1*	*DDX47*	DEAD (Asp-Glu-Ala-Asp) box polypeptide 47
IV	C37F5.1	*lin-1*	*ELK3*	ETS-Domain Protein (SRF Accessory Protein 2)
IV	H34C03.2	*H34C03.2*	*USP4*	ubiquitin specific peptidase 4
V	F22F7.2	*F22F7.2*	*SCCPDH*	saccharopine dehydrogenase (putative)
V	W02H5.4	*W02H5.4*	POGK	pogo transposable element with KRAB domain
V	H14N18.1	*unc-23*	*BAG2*	BCL2-associated althanogene 2
V	ZK856.10	*ZK856.10*	*POLR3H*	pol (RNA) III (DNA directed) polypep. H (22.9kD)
X	F13D11.2	*hbl-1*	*ZNF124*	zinc finger protein 124
X	K09E2.1	*K09E2.1*	*COL6A6*	collagen, type VI, alpha 6
X	T27B1.2	*ztf-19*	*PRDM10*	PR domain containing 10
Nematode-Specific				
IV	F38A5.6	*F38A5.6*	N/A	Unknown
IV	F38E11.9	*F38E11.9*	N/A	Unknown
IV	C43F9.4	*C43F9.4*	N/A	Unknown
IV	W02A2.8	*W02A2.8*	N/A	Unknown
V	Y45G12C.14	*srj-19*	N/A	serpentine receptor, class J
V	ZK697.4	*sri-27*	N/A	serpentine receptor, class I
V	ZC317.6	*ZC317.6*	N/A	Unknown
X	C24H10.1	*C24H10.1*	N/A	claudin homolog

Figure S2 related to Figure 2. Genome-wide RNAi screen identifies conserved mesodermal factors that suppress ectopic epithelial cell division. **(A)** Experimental workflow of the genome-wide mesoderm-specific RNAi screen. **(B)** The 39 genes identified by mesoderm-specific RNAi screen are grouped based on annotated functions. Chr., chromosome.

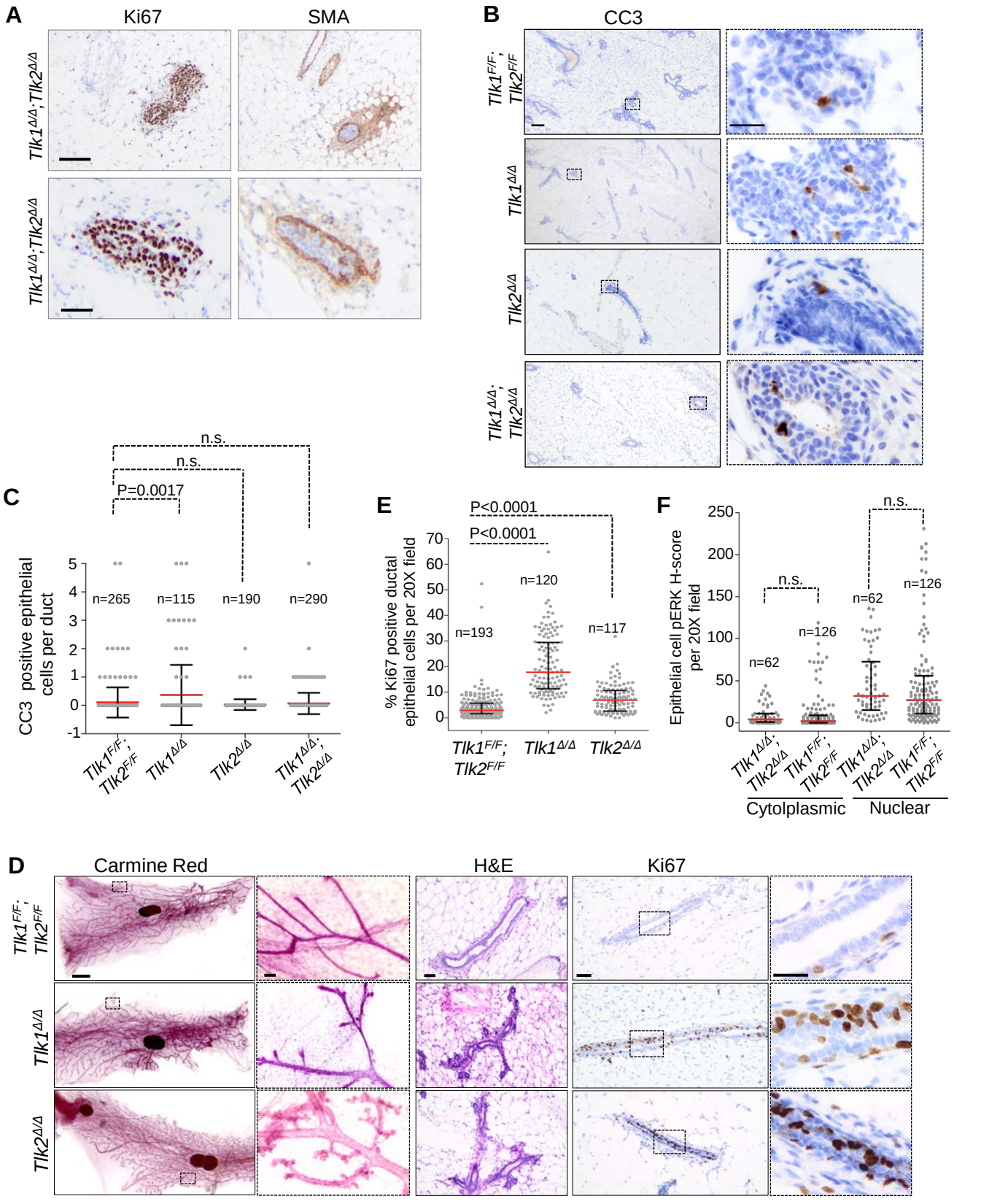
A
Ki67
SMA
Tlk1Δ/Δ;Tlk2Δ/Δ
Tlk1Δ/Δ;Tlk2Δ/Δ
B
CC3
Tlk1F/F; Tlk2F/F
Tlk1Δ/Δ
Tlk2Δ/Δ
Tlk1Δ/Δ; Tlk2Δ/Δ
C
n.s.
n.s.
P=0.0017
CC3 positive epithelial cells per duct
n=265
n=115
n=190
n=290
Tlk1F/F; Tlk2F/F
Tlk1Δ/Δ
Tlk2Δ/Δ
Tlk1Δ/Δ; Tlk2Δ/Δ
E
P<0.0001
P<0.0001
% Ki67 positive ductal epithelial cells per 20X field
n=193
n=120
n=117
Tlk1F/F; Tlk2F/F
Tlk1Δ/Δ
Tlk2Δ/Δ
F
n.s.
n.s.
Epithelial cell pERK H-score per 20X field
n=62
n=126
n=62
n=126
Tlk1Δ/Δ; Tlk2Δ/Δ
Tlk1F/F; Tlk2F/F
Tlk1Δ/Δ; Tlk2Δ/Δ
Tlk1F/F; Tlk2F/F
Cytolplasmic
Nuclear
D
Carmine Red
H&E
Ki67
Tlk1F/F; Tlk2F/F
Tlk1Δ/Δ
Tlk2Δ/Δ

Figure S3 related to Figure 4. *In vivo* deletion of *Tlk1/2* in mouse mammary fibroblasts increases the proliferation of adjacent epithelial cells. (A) Examples of sections from *Fsp-cre*;$Tlk1^{F/F}$;$Tlk2^{F/F}$ ($Tlk1^{\Delta/\Delta}$;$Tlk2^{\Delta/\Delta}$) mice immune-stained with Ki67 or smooth muscle actin (SMA) and counterstained with hematoxylin (blue) (top, bar = 100 µm; bottom, bar = 50 µm). **(B)** Representative images of sections of inguinal mammary gland from $Tlk1^{F/F}$;$Tlk2^{F/F}$ mice (control), $Tlk1^{\Delta/\Delta}$, $Tlk2^{\Delta/\Delta}$ or $Tlk1^{\Delta/\Delta}$;$Tlk2^{\Delta/\Delta}$ mice immuno-stained for cleaved caspase-3 (CC3; brown) and counterstained with hematoxylin (blue) (bar = 50 µm). Boxes indicate area of magnification in adjacent panel (bar = 20 µm). **(C)** Number of CC3 positive cells per duct (dots) of tissue described in (B). Red bar, mean; black bars, S.D.; pooled counts from 2 mice of each genotype; n.s., not significant. P value: Student's t-test. **(D)** Left: Bright field images of whole mount inguinal mammary glands from 10-week-old $Tlk1^{F/F}$;$Tlk2^{F/F}$(control), *Fsp-cre*;$Tlk1^{F/F}$ ($Tlk1^{\Delta/\Delta}$) and $Tlk2^{\Delta/\Delta}$ mice stained with carmine red (bar = 2000 µm). Boxes indicate area of magnification in adjacent panel (bar = 100 µm). Middle: H&E stained sections of opposite inguinal gland (bar = 50 µm). Right: representative images of sections of inguinal mammary glands immuno-stained for Ki67 (brown) and counterstained with hematoxylin (blue) (bar = 50 µm). Boxes indicate area of magnification in adjacent panel (bar = 20 µm). **(E)** Percent Ki67 positive epithelial cells per 20X field (dots) of tissue sections described in (A). Red bar, median; black bars, interquartile range; pooled counts from 6 control mice or 3 and 5 mice for the $Tlk1^{\Delta/\Delta}$ and $Tlk2^{\Delta/\Delta}$ groups respectively. P value: Mann-Whitney test of medians. **(F)** Quantification of phospho-ERK (pERK) positive epithelium from both cytoplasmic and nuclear signal per 20X field (dots). Red bar, median; black bars, interquartile range; pooled counts from 3 control or 5 $Tlk1^{\Delta/\Delta}$;$Tlk2^{\Delta/\Delta}$ mice. P value: Mann-Whitney test of medians.

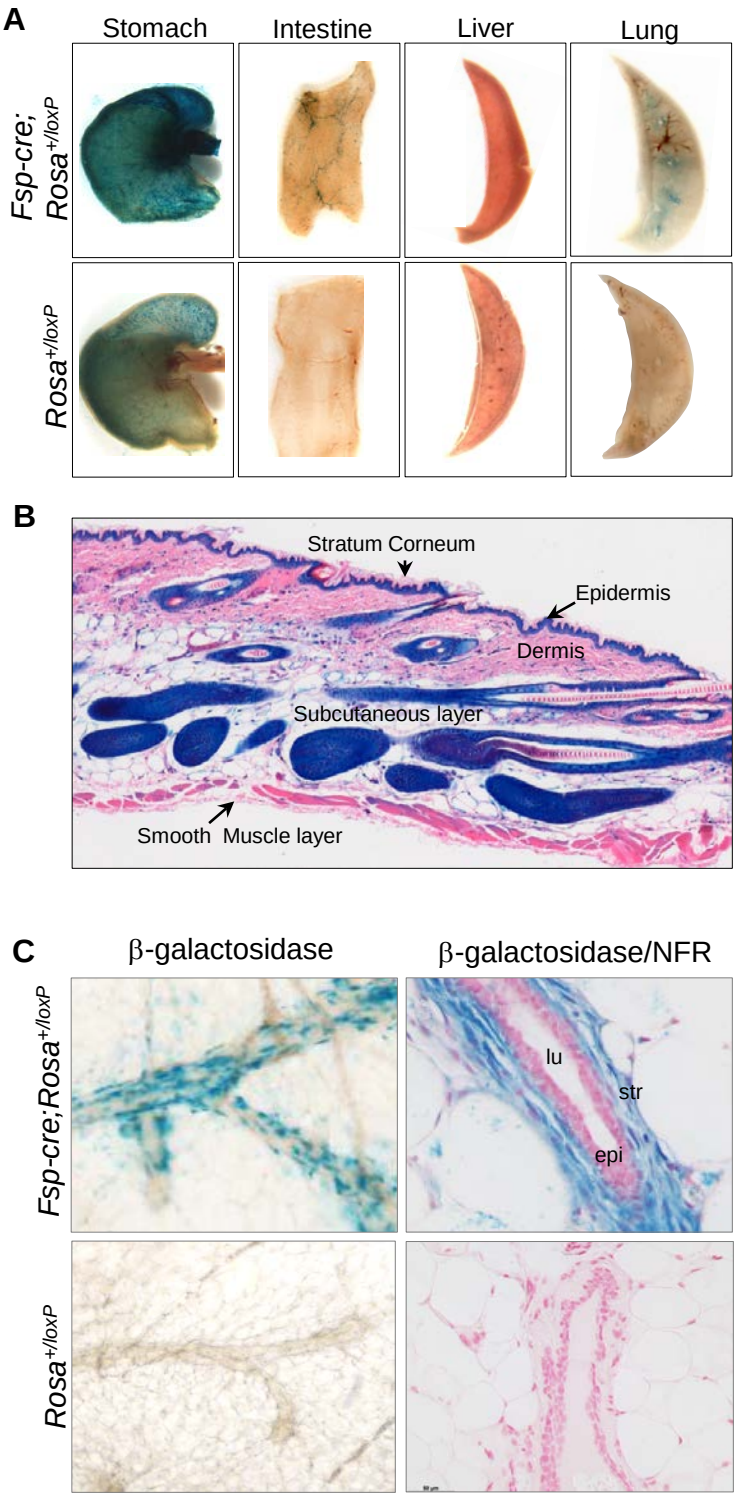
A
Stomach
Intestine
Liver
Lung
Fsp-cre; Rosa+/loxP
Rosa+/loxP
B
Stratum Corneum
Epidermis
Dermis
Subcutaneous layer
Smooth Muscle layer
C
β-galactosidase
β-galactosidase/NFR
Fsp-cre;Rosa+/loxP
Rosa+/loxP
lu
str
epi

Figure S4 related to Figure 4 and Figure 5. *Fsp-cre* transgene expression in various tissues. (A) Organs and glands were isolated from the fsp –cre line possessing only the RosaloxP reporter, fixed and stained for conditional β-galactosidase reporter activity in situ. Staining of the stomach is from intestinal bacteria as evidenced by the control while minimal staining was observed in the liver, lung, and intestine with most if not all staining from connective tissue and associated with the vasculature. **(B)** In situ X-gal staining of skin from a Fsp-cre;$Rosa^{+/loxP}$ mouse, that was then paraffin embedded and sectioned. -cre expression was detected in every cell type in the skin: Adipocytes, Smooth Muscle, Epithelium and Stroma. **(C)** Higher (10x) magnification of wholemount mammary glands from Figure 4J from mice with the indicated genotypes; cross sections stained for β-galactosidase and counterstained with nuclear fast red (NFR, bottom panels). Str, stromal fibroblasts; lu, lumen; epi, epithelial cells.

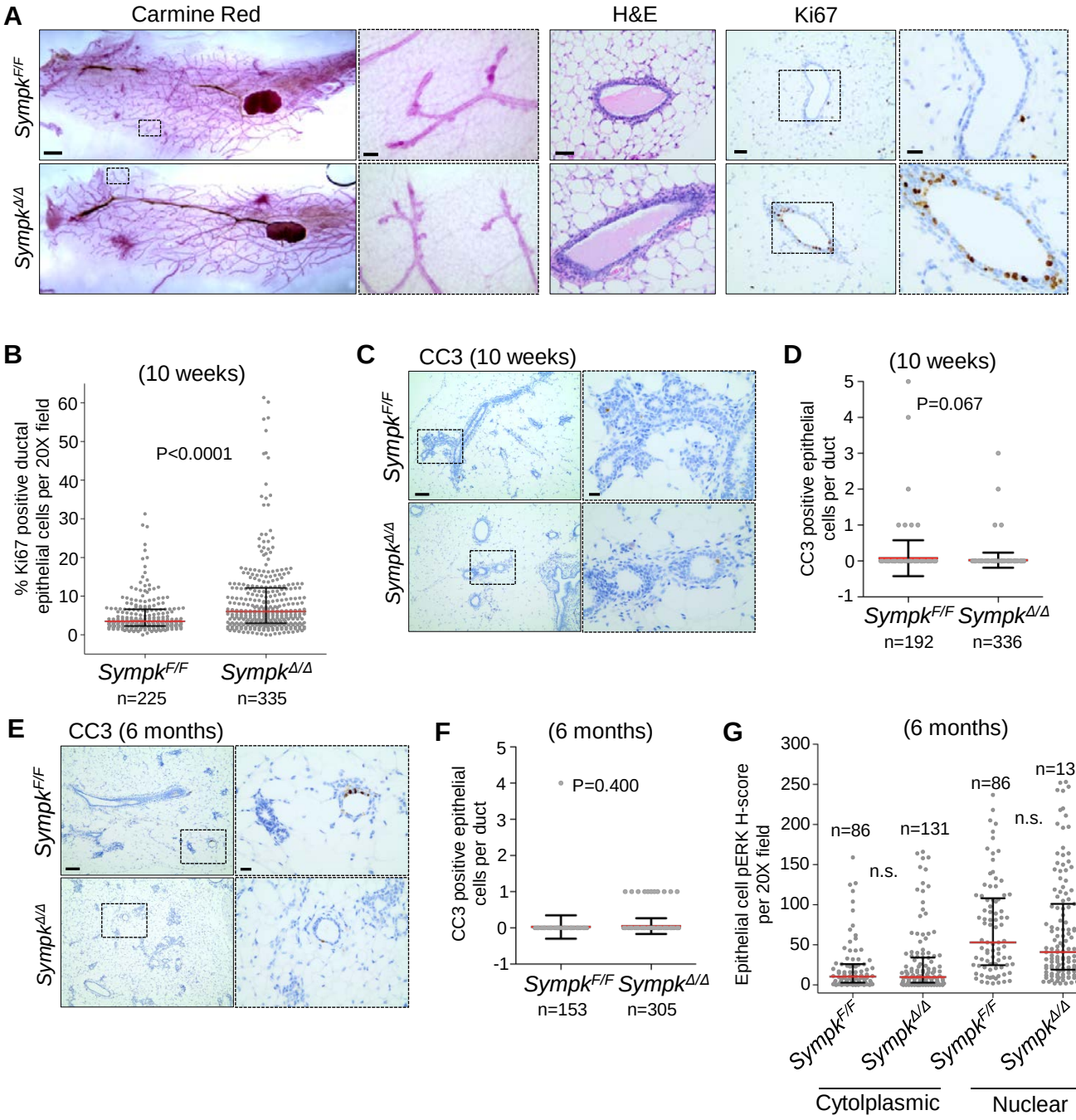
A
Carmine Red
H&E
Ki67
Sympk F/F
Sympk Δ/Δ
B
(10 weeks)
% Ki67 positive ductal epithelial cells per 20X field
P<0.0001
Sympk F/F
Sympk Δ/Δ
n=225
n=335
C
CC3 (10 weeks)
Sympk F/F
Sympk Δ/Δ
D
(10 weeks)
CC3 positive epithelial cells per duct
P=0.067
Sympk F/F
Sympk Δ/Δ
n=192
n=336
E
CC3 (6 months)
Sympk F/F
Sympk Δ/Δ
F
(6 months)
CC3 positive epithelial cells per duct
P=0.400
Sympk F/F
Sympk Δ/Δ
n=153
n=305
G
(6 months)
Epithelial cell pERK H-score per 20X field
n=86
n.s.
n=131
n=86
n.s.
n=131
Sympk F/F
Sympk Δ/Δ
Sympk F/F
Sympk Δ/Δ
Cytolplasmic
Nuclear

Figure S5 related to Figure 5. *In vivo* deletion of *Sympk* in mouse mammary fibroblasts increases proliferation of adjacent ductal epithelium. (A) Left: bright field images of whole mount inguinal mammary glands from 10-week-old $Sympk^{F/F}$ mice (control) or $Fsp\text{-}cre;Sympk^{F/F}$ ($Sympk^{\Delta/\Delta}$) mice stained with carmine red to emphasize ductal branching (bar = 1000 µm). Boxes indicate area of magnification in adjacent panel (bar = 100 µm). Middle: H&E stained sections of opposite inguinal gland (bar = 50 µm). Right: representative images of sections of inguinal mammary gland immuno-stained for Ki67 (brown) and counterstained with hematoxylin (blue) (bar = 50 µm). Boxes indicate area of magnification in adjacent panel (bar = 20 µm). **(B)** Percent Ki67 positive epithelial cells per 20X field (dots) of tissue sections described in (A). Red bar, median; black bars, interquartile range; pooled counts from 6 control mice or 7 mice for the *Fsp-cre* group. P value: Mann-Whitney test of medians. **(C&E)** Representative images of sections of inguinal mammary gland from 10-week **(C)** or 6-month-old **(E)** $Sympk^{F/F}$ or $Sympk^{\Delta/\Delta}$ mice immuno-stained for cleaved caspase-3 (CC3; brown) and counterstained with hematoxylin (blue) (bar = 50 µm). Boxes indicate area of magnification in adjacent panel (bar = 20 µm). **(D&F)** Number of CC3 positive cells per duct (dots) of tissue described in (C) or (E) respectively. Red bar, mean; black bars, S.D.; pooled counts from 2 mice of each genotype. P value: Student's t-test. **(G)** Quantification of phospho-ERK (pERK) positive epithelium from both cytoplasmic and nuclear signal per 20X field (dots). Red bar, median; black bars, interquartile range; pooled counts from 4 $Sympk^{F/F}$ or 5 $Sympk^{\Delta/\Delta}$ 6-month-old mice. P value: Mann-Whitney test of medians. n.s., not significant.

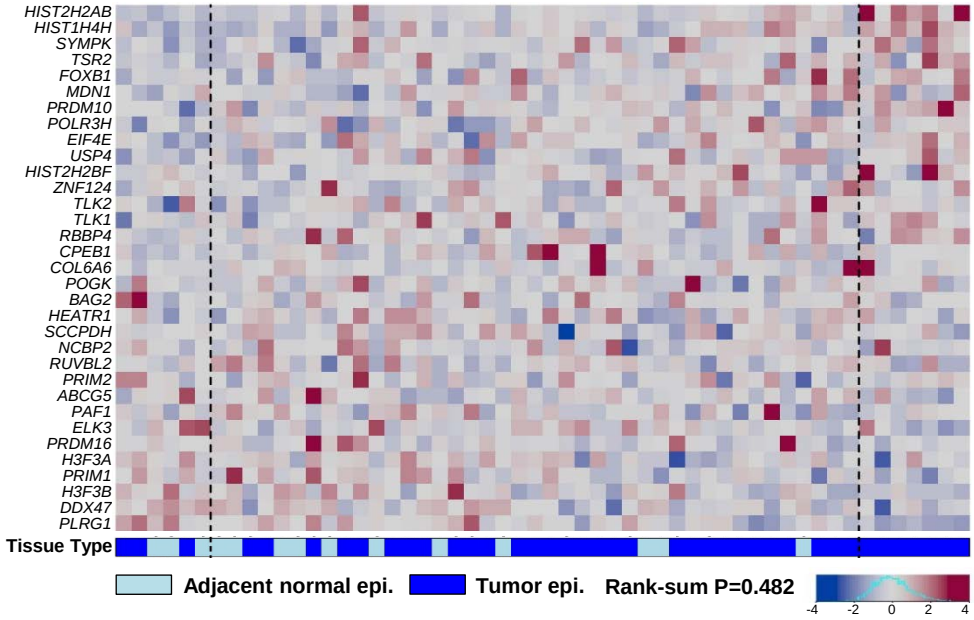
HIST2H2AB
HIST1H4H
SYMPK
TSR2
FOXB1
MDN1
PRDM10
POLR3H
EIF4E
USP4
HIST2H2BF
ZNF124
TLK2
TLK1
RBBP4
CPEB1
COL6A6
POGK
BAG2
HEATR1
SCCPDH
NCBP2
RUVBL2
PRIM2
ABCG5
PAF1
ELK3
PRDM16
H3F3A
PRIM1
H3F3B
DDX47
PLRG1
Tissue Type
Adjacent normal epi.
Tumor epi.
Rank-sum P=0.482
-4
-2
0
2
4

Figure S6 related to Figure 6. The human ortholog signature fails to distinguish breast tumor epithelium from adjacent normal epithelium. Heatmap displaying RNA expression of the 33 human orthologs in normal (n=14) and tumor epithelium (n=40) from breast cancer patients. Each sample was given a rank for each gene and ordered among the experimental samples according to the rank-sums. The boundaries (dashed lines) represent the 95% distribution limits for rank-sums of 10,000 randomly generated samples. The P value indicates the ability of the gene signature to distinguish normal from tumor epithelium in breast cancer patients. Epi., epithelium. See also Table S4.

A

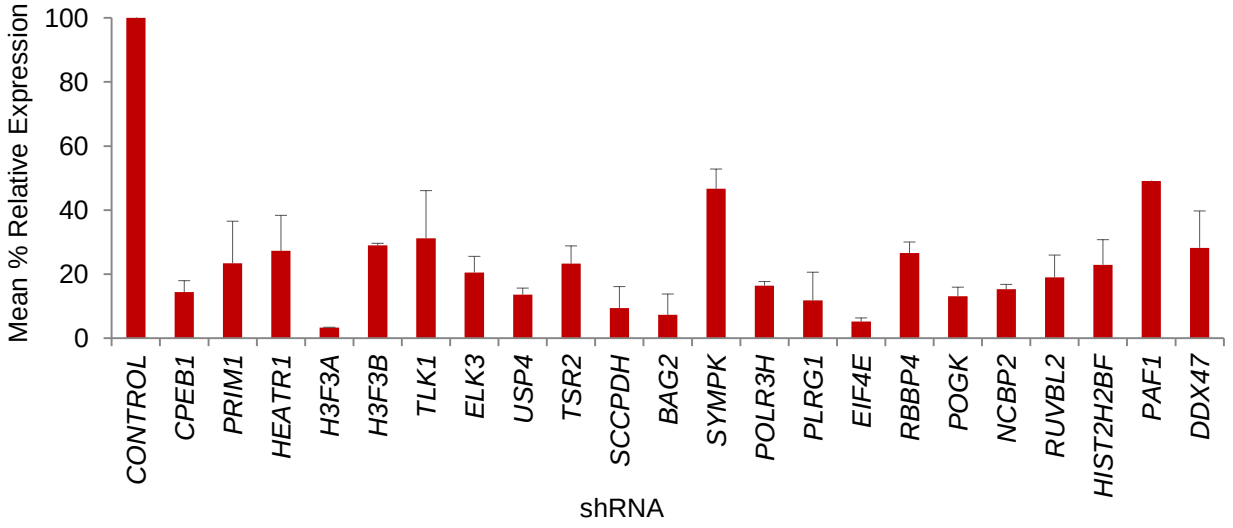

B

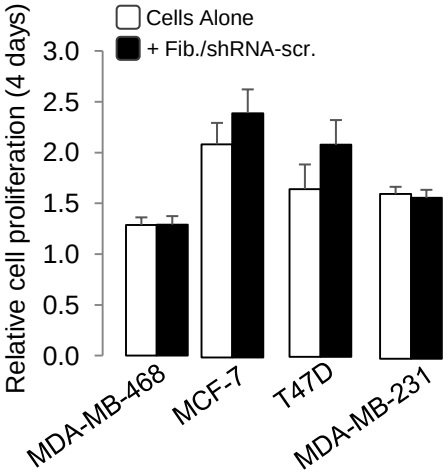

C

Mutation status of breast cancer cell lines (x = no mutation)				
	RTK	Ras	Raf	NF1
MDA-468	DDR2 (V824A) missense EPHB6 (G403D) missense ERBB2 (G152fs) frame-shift	x	x	(Q1033R) missense
MCF-7	EPHA5 (L1009P) missense ERBB4 (Y1242C) missense	x	x	x
T47D	x	x	x	x
MDA-231	PDGFRA (Y172F) missense	KRAS (G13D) missense	BRAF (G464V) missense	(L466fs) frame-shift
BT474	x	x	x	x
MCF10A	x	x	x	x

Figure S7 related to Figure 7. Characterization of cells used in human co-culture experiments (A) 22 human orthologs were knocked down by lentirviral shRNA transduction as determined by real-time quantitative PCR analysis. Data are shown as mean percent residual gene expression ± standard deviation relative to non-silencing shRNA and normalized with *GAPDH* expression. **(B)** Fold increase in cell number at day 4 of culturing for breast cancer cell lines alone or co-cultured with shRNA control (shRNA-scr.) infected fibroblasts (Fib.). n=3 independent experiments with each experiment performed in triplicate. Data are presented as average ±SEM. See also Table S3. **(C)** Mutation status of breast cancer cell lines from Broad-Novartis Cancer Cell Line Encyclopedia (CCLE) https://portals.broadinstitute.org/ccle/home.